WITHDRAWN: Changing the morphology of biofilm materials to improve the simultaneous nitrification and denitrification stability of rotating biological contactors with seasonal changes

Cheng Gao
Sichuan University - Wangjiang Campus: Sichuan University
Yi Chen
Sichuan University - Wangjiang Campus: Sichuan University
Tianqi Ao
Sichuan University
Qingpeng Guo
Sichuan University
wenqing Chen
1572141922@qq.com

Sichuan University - Wangjiang Campus: Sichuan University

Research Article

Keywords: Rotating biological contactors, temperature change, simultaneous nitrification and denitrification, material

Posted Date: April 12th, 2022

DOI: https://doi.org/10.21203/rs.3.rs-1430351/v1

EDITORIAL NOTE:

The full text of this preprint has been withdrawn by the authors while they make corrections to the work. Therefore, the authors do not wish this work to be cited as a reference. Questions should be

directed to the corresponding author.

Abstract

Rotating biological contactors (RBCs) have the advantages of simple operation, low sludge output, small footprint, and low operating cost and have been extensively studied. This study investigated the pollutant removal effects of two polyethylene materials with different specific surface areas and pore structures (flat and cylindrical) in RBC low-temperature operation. The results of 16S amplicon sequencing showed that fillers with porous channels and a large specific surface area can improve the stability of the microbial community structure and the simultaneous nitrification and denitrification (SND) efficiency of RBCs with seasonal changes. Under low-temperature (10°C) operating conditions, the removal efficiencies of the flat, porous D material for chemical oxygen demand (COD), ammonia nitrogen and total nitrogen were 74%, 60%, and 55%, respectively. The removal efficiencies of the cylindrical single-hole X material for COD, ammonia nitrogen, and total nitrogen were 48%, 38%, and 35%, respectively. The results are of great significance for the practical application of RBCs, especially in low-temperature environments.

Introduction

Freshwater resources are an important foundation for human survival and development. Human activities such as urbanization have caused considerable damage to freshwater resources. Excessive discharge of nitrogen into water bodies will cause cyanobacterial blooms, destroying the water ecosystem. Therefore, the treatment of urban domestic sewage is important and valuable.

Traditional nitrification and denitrification processes are usually carried out in different bioreactors or use different aeration intervals; in contrast, simultaneous nitrification and denitrification (SND) processes remove nitrogen in the same reactor under specific operating conditions and require less input of oxygen and carbon sources (Xia et al., 2019). Sequencing batch reactors (SBRs), membrane bioreactors (MBR), sequencing batch airlift reactors (SBARs), fluidized bed biofilm reactors, moving bed biofilm reactors (MBBRs), etc. can realize SND. However, these reactors have the disadvantages of poor shock load resistance and large sludge output (Geng et al., 2020; Teng et al., 2020; Bassin et al., 2018). Among these reactors, the rotating biological contactor (RBC) has the advantages of simple operation, low sludge output, small footprint, low maintenance cost and low operating cost and has been extensively studied (Han et al., 2019; Waqas et al., 2021). The filling material in the RBC reaction tank has evolved from a few rotating discs to a large number of light and tiny filler particles, which are used to increase the film quantity and the effective contact area between sewage and microorganisms (Waqas et al., 2019; Waqas et al. al., 2021). In RBCs, the complex interaction of artificial substrates and related microbial communities can treat various types of sewage, and nitrification and denitrification processes can be regulated by controlling the speed of the machine and the degree of flooding (Kiran et al., 2017; Spasov et al., 2020). RBCs can realize SND through intermittent contact with the air and flooding of the biofilm (Bhattacharya et al., 2021).

At present, most of the research on RBCs focuses on optimizing their operating parameters to improve their decontamination ability. Li et al. (2019) implemented a laboratory-scale rotary drum biological

contactor (RDBC) and studied its abiotic oxygen transfer rate and treatment capacity for domestic sewage treatment. The results showed that the rotary drum rotation speed and immersion degree of the biofilm have a great influence on the dissolved oxygen (DO) transfer efficiency. The dominant bacteria in the biofilm were *Nitrosomonas europaea* and Kuenenia, indicating that aerobic and anammox bacteria jointly lead to denitrification. Dong et al. (2021) studied the optimal process conditions for the removal of total chemical oxygen demand (COD), total nitrogen and ammonia nitrogen from salt-bearing mustard wastewater (MTWW) by a packed cage RBC system with an organic load of 26.71 kg/d. The lowest energy consumption was obtained with a rotating disk speed of 1.62 rpm (7.62 m/s) and immersion rate of 46%. However, RBC reactors generally suffer from poor denitrification efficiency under low-temperature operating conditions. Temperature is the most important factor affecting the stability of the microbial community structure and denitrification performance. Temperature drives changes in microbial community structure, mainly due to the different sensitivities and tolerances of microorganisms at different temperatures (chen et al., 2017, Siripong et al., 2007). Through bioenhancement and optimization of operating parameters, the processing performance under low-temperature operation can be improved. In the bioaugmentation method, pure cultures or mixed cultures that were initially screened or enriched in the wastewater system are typically added. Ma et al. (2019) explored the potential of simultaneous removal of phenol and nitrogen from coal gasification wastewater (CGW) and established an SND biological enhancement system using Pseudomonas sp. HJ3 as a bacterium to promote coal gasification and achieve simultaneous removal of phenol and nitrogen in wastewater treatment. Iannacone et al. (2020) regulated the performance of simultaneous partial nitrification and denitrification in a continuous flow intermittent aeration MBBR by adding a carbon source. The results showed that adding acetic acid to the wastewater was beneficial to the diversity of microbial communities, while increasing C/N by increasing ethanol resulted in an overgrowth of heterotrophic bacteria. DO control can effectively regulate the microbial community structure. Hocaoglu et al. (2011) studied the effect of low DO on the SND of black water in an MBR, and the results showed that nitrate was completely removed at low DO levels. However, when DO increased to 0.5 mg/L, the removal rate gradually decreased. Increasing the pH value is an effective way to change the community structure of nitrifying bacteria and increase the rate of nitrification. Feng et al. (2008) studied the denitrification effect of SBR treatment of low-carbon synthetic wastewater under different pH conditions, and the results showed that the neutral to slightly alkaline pH range is beneficial to SND in SBRs. Reasonable control of the hydraulic retention time (HRT) can improve the performance of reactors at low temperature. Wang et al. (2020) studied the effect of different biological factors on the SND performance in a moving bed SBR. The results showed that the extension of HRT strongly affected the growth of nitrifying bacteria, resulting in a high level of COD consumption and weakening the denitrification process of the biological system. However, these control methods have the disadvantages of high cost and complicated control processes. Therefore, a simple method is urgently needed to solve the problem of poor denitrification performance of bioreactors at low temperature.

This study proposes a new strategy to change the morphology of loaded biofilm materials that enhances the adaptability of microorganisms at low temperatures and reduces the interaction between

microorganisms. Therefore, such changes can enhance the stability of the microbial community structure and of SND performance with seasonal changes. This study explored the pollutant removal effects of two polyethylene fillers with different specific surface areas and pore structures (flat and cylindrical) in RBCs to improve the overall stability of RBC denitrification efficiency with seasonal changes. The results of this study show that changing the morphology of the filling material can significantly improve the stability of the microbial community structure and of SND, which is of great significance to the practical application of RBCs.

Materials And Methods

2.1 RBC equipment

A schematic diagram of the experimental device is shown in Fig. A.1. The experimental device was based on an RBC designed and manufactured by the Sichuan Haote Industrial Group. The equipment components included the reaction tank, rotating shaft, hollow drum, AC motor, speed regulator, filling materials, water inlet and water outlet. The reaction tank consisted of a semicylindrical groove with a radius of 0.24 m and a length of 0.56 m; the hollow drum was a hollow cylinder welded out of steel plates with round holes and had a radius of 0.2 m and a length of 0.5 m; and the filling materials were PVC plastic that had been manually screened out. Movement was driven by a motor that rotated the hollow drum at a constant speed in a fixed direction; the hollow drum then further drove the internal biological filler to move in a fixed direction. Biological fillers achieved the degradation of pollutants during alternating contact with air and sewage.

During the operation of the equipment, attached biofilms were continuously shed and renewed due to their own motion, mutual friction and shear force from the movement of the water body. During the experiment, the influent sewage solution was prepared from tap water and stored in a water distribution tank. It was transported by a peristaltic pump to the inlet of the reaction tank. After the microorganisms attached to the biological filler materials were degraded, they finally flowed out from the outlet of the reaction tank.

2.2 Experimental operating parameters

The experimental operating parameters are shown in Table 1. Submergence in excess of 50% will decrease the rate of oxygen transfer in the system. An HRT that is too short will result in low removal rates, whereas an HRT that is too long will not be economically feasible. A significant advantage of full-scale RBCs is that they require short HRTs (generally less than 1 h) (Cortez et al., 2008). The experiment used two RBCs of the same size made by the Sichuan Haote Industrial Group. One reactor drum was filled with D-type biological filler, and the other reactor drum was filled with X-type biological filler. The D material had a 64-hole structure with a specific surface area of 400 m^2/m^3, and the X material had a 4-hole structure with a specific surface area of 350 m^2/m^3. Both biological fillers were made of PVC. The

two materials were both cylindrical but had different thicknesses. The porous D material had a thickness of 0.4 mm, and the less porous X material had a thickness of 1.2 mm.

Table 1
Specific operating parameters

Material	Fill rate	Rotating speed	Immersion ratio	Hydraulic retention time	Temperature
D	80	3 r/min	50%	1 h	5 ~ 30℃
X					

2.3 Test water and water quality determination

In the experiment, artificially configured domestic sewage was used, in which glucose, ammonium chloride, and potassium dihydrogen phosphate were used as the carbon source, nitrogen source and phosphorus source, respectively. Calcium chloride, magnesium sulfate and trace element solution were added to the artificial sewage as a source of trace substances required for the growth and reproduction of microorganisms. Sodium hydroxide was used to adjust the acidity and alkalinity of the artificial sewage. The simulated wastewater was configured according to domestic sewage standards (Li et al., 2020; Gao et al., 2020). The composition of the wastewater was as follows: COD 250 ± 2 mg L^{-1}; NH_4^+-N, 15 ± 0.14 mg L^{-1}; phosphates, 3 mg L^{-1}; $CaCl_2$ and $MgSO_4$, 0.2 mg L^{-1}. The inlet was operated with continuous flow. Sampling in Sichuan started in September (autumn) and stopped in December (winter). Sampling at the inlet and outlet of the system started after 140 days of system operation. The water quality parameters COD, $NH4^+$-N, and TN were measured according to standard methods (Luo et al., 2020).

2.4 Hanging film

The inoculated activated sludge used in the experiment was return sludge from the secondary sedimentation tank of the Chengdu Key Wastewater Treatment Plant. The inoculated sludge was dark brown, with good settling and agglomeration properties. Microscopic observation of the sludge before inoculation revealed abundant biological phases in the inoculated sludge. Many indicator organisms, such as Vorticella, Araliacea, and Rotifera, were present, and they were very active. At the beginning of system operation, 17 L of inoculated activated sludge was added to the reaction tank of the RBC for 24 hours, and then, artificial domestic sewage was added until the liquid level of the mixed liquid reached the water outlet. After 24 hours, the operation was stopped, the mixture was allowed to stand for sedimentation, and the supernatant was drained. Then, artificial domestic sewage was continuously added for 12 hours, the mixture was allowed to stand to settle, and the supernatant and approximately one-third of the suspended sludge were discharged; this procedure was repeated until all the suspended sludge was discharged. When all the suspended sludge had been discharged, the RBC operated in continuous flow mode until the biofilm was basically mature. Fifteen days after film hanging began, a light yellow biofilm appeared on the surface of the biological filler and gradually thickened. After one month of continuous operation, there was a clearly visible brown covering inside the drum with a certain

thickness, indicating that the biofilm had basically matured and that RBC film coating had been completed (Zhong et al., 2021).

2.5 DNA sampling

A total of 18 samples were taken during the experiment, and the sample numbers and sampling times are shown in Table 2. The microbial samples were collected after the RBC reactor had successfully started and operated continuously for 140 days. To improve the representativeness of the samples relative to the reactor, the sampling points along the biological filler were evenly arranged according to the shape of the biological drum. Three samples were taken on the upper, middle, lower, left and right parts of the drum and mixed together. The sampling interval was 10 days, and the collected sample volume was 50 cm^3 (calculated based on the volume of the biological filler). After the samples were collected, they were stored in a refrigerator at -70°C for later DNA extraction. For DNA extraction, the sample was placed in a sterile bottle, 5 ml saline (0.9% NaCl) was added, and the sample was shaken for 1 minute, sonicated for 3 minutes, and finally centrifuged at 3000 r for 5 minutes to collect the biofilm suspension. The above operation was repeated three times.

Table 2
Sample numbers and sampling times

Operating days (d)	140	150	160	170	180	190	200	210	220
D	D1	D2	D3	D4	D5	D6	D7	D8	D9
X	X1	X2	X3	X4	X5	X6	X7	X8	X9

2.6 High-throughput sequencing

One gram of fresh biofilm sample was weighed, and a DNeasy-PowerSoil kit (QIAGEN, Netherlands) was used to extract the total DNA of the microbial genome according to the manufacturer's instructions. The V3–V4 region of the bacterial 16S RNA gene was amplified by PCR; the upstream primer sequence was ACTCCTACGGGAGGCAGCA, and the downstream primer sequence was GGACTACHVGGGTWTCTAAT. Sample-specific 7-bp barcodes were incorporated into the primers for multiplex sequencing. PCR amplicons were purified with Agencourt AMPure Beads (Beckman Coulter, Indianapolis, IN) and quantified using the PicoGreen dsDNA Assay Kit (Invitrogen, Carlsbad, CA, USA). After the individual quantification step, amplicons were pooled in equal amounts, and paired-end 2×300 bp sequencing was performed using the Illumina MiSeq platform with MiSeq Reagent Kit v3 at Shanghai Personal Biotechnology Co., Ltd. (Shanghai, China) (Franco-Frías et al., 2021).

2.7 Data analysis

The Quantitative Insights Into Microbial Ecology (QIIME, v1.8.0) pipeline was employed to process the sequencing data, as previously described. Sequence data analyses were mainly performed using QIIME and R packages (v3.2.0). Operational taxonomic unit (OTU)-level alpha diversity indexes, such as the

Chao1 richness estimator, ACE metric (abundance-based coverage estimator), Shannon diversity index, and Simpson index, were calculated using the OTU table in QIIME. Conoco was used for principal component analysis (PCA). The circlize package in the R language was used to draw the relative abundance map; the ggalluvial data package was used to draw the impact map; the correlation calculation was completed by the psych package; values with $P < 0.5$ were extracted; the heatmap was provided by the pheatmap package Draw; and the network correlation diagram was completed by Cytoscape software. Linear discriminant analysis (LDA) effect size (LEfSe) was performed on the website http://huttenhower.sph.harvard.edu/galaxy/ (Wang et al., 2017; Lin et al., 2019).

Results And Discussion

3.1. Analysis of COD removal and nitrogen removal efficiency

The outlet water quality is shown in Fig. 1. The experimental results show that the properties of the two materials are greatly affected by temperature. In general, the removal of COD, ammonia nitrogen and total nitrogen by the D material was considerably better than that of the X material. When the temperature was 25°C, the removal efficiencies of the D material for COD, ammonia nitrogen and total nitrogen were 94%, 98% and 78%, respectively. As the temperature dropped to 10°C, the removal efficiency of COD, ammonia nitrogen, and total nitrogen by the D material gradually decreased to 74%, 60%, and 55%, respectively. When the temperature was 25°C, the removal efficiency of the X material for COD, ammonia nitrogen and total nitrogen was 90%, 97% and 73%, respectively. As the temperature dropped to 10°C, the removal efficiency of COD, ammonia nitrogen and total nitrogen by the D material gradually decreased to 48%, 38%, and 35%, respectively.

In short, as the temperature decreased, the removal efficiency of the two fillers for COD, ammonia nitrogen, and total nitrogen also decreased, but the degree of decrease of the D filler was lower, showing more stable denitrification performance. The low temperature in winter reduces the biological activity of microorganisms and the growth rate of microorganisms, resulting in a reduction in the removal rates of COD, ammonia nitrogen, and total nitrogen. There may be two main reasons for the effect of low temperature on denitrification performance, namely, biological activity and microbial growth rate (Yang et al., 2015; Li et al., 2016; Wang et al., 2017). The research results of Yuan et al., 2018 showed that the ammonia oxidation rate and nitrite oxidation rate increase nonlinearly with temperature, which conforms to the Hoff-Arrhenius model. This is mainly because temperature affects biological deaminase activity, such as AMO activity. Dawson et al., 1972 showed that the denitrification rate increases nonlinearly with temperature, which is similar to the Arrhenius temperature relationship. The comparison of the two fillers showed that the D filler exhibits better environmental adaptability.

3.2 Microbial diversity

3.2.1 Microbial community alpha diversity

The microbial diversity indexes of each sample are shown in Table 3. The Shannon and Simpson indexes are used to quantify community diversity, and the Chao and Ace indexes are used to quantify community richness (Zhimiao et al., 2019, Bai et al., 2015; Xie et al., 2018). Regarding the alpha diversity analysis, the Shannon, Simpson, Chao and Ace indexes of each sample are shown in Table 1. The Shannon, Simpson, Chao and Ace indexes of the bacteria on material D were all greater than those of material X, which indicates that the microbial community diversity and community richness of material D were greater than those of material X.

Table 3
Microbial diversity indexes for each sample

	Simpson	Chao1	ACE	Shannon
D1	0.950951	1137.12	1095.91	6.57
D2	0.954713	1131.83	1177.00	6.80
D3	0.942475	1341.81	1424.70	7.05
D4	0.976262	1416.58	1420.60	7.35
D5	0.959901	881.00	881.36	6.70
D6	0.962047	1037.19	1067.11	6.87
D7	0.971880	1232.34	1292.77	7.13
D8	0.963600	1078.00	1078.00	7.20
D9	0.938239	1256.86	1266.44	6.33
X1	0.915683	763.17	745.00	5.78
X2	0.646376	414.33	454.04	2.69
X3	0.783746	454.97	487.95	3.88
X4	0.831254	559.76	577.31	4.57
X5	0.912979	693.11	729.89	5.30
X6	0.960721	822.64	855.69	6.39
X7	0.887547	727.81	729.53	5.04
X8	0.934098	808.32	845.33	5.77
X9	0.899148	810.63	792.94	5.30

The PCA results for the microbial diversity of each sample are shown in Fig. A.2. The PCA of the four indicators showed that the first two principal components (PCs) accounted for 99.8% of the total variance of the original data set. The explanation rate of PC1 for the total variance was 97.53%, and the

explanation rate of PC2 for the total variance was 2.23%. PC1 indicates that the diversity and abundance of bacterial communities are mainly related to the nature of the material.

The results of correlation analysis between the microbial diversity indexes and environmental factors (Table A.1) are shown in Fig. A.2 and Table 4. Spearman correlation analysis showed that the Chao1, ACE and Shannon indexes of bacteria had a significant positive correlation with the specific surface area and number of pores of the materials. This correlation indicates that the more pores there are and the greater the specific surface area is, the greater the richness and diversity of the microbial community.

Table 4
Correlation analysis of the microbial diversity indexes and environmental factors for each sample

Diversity index	Environmental Factors	R	P
Simpson	Number of holes	0.76	0
Chao1	Number of holes	0.87	0
ACE	Number of holes	0.87	0
Shannon	Number of holes	0.85	0
Simpson	Specific surface area	0.76	0
Chao1	Specific surface area	0.87	0
ACE	Specific surface area	0.87	0
Shannon	Specific surface area	0.85	0

3.2.2 Analysis of the beta diversity of the microbial community

The PCA results for all genera and functional bacteria are shown in Fig. 2. PCA was used to analyse the changes in microbial genera and functional bacterial composition between different treatments. The results showed that there were significant differences in the functional diversity of the microbial communities between the different treatments. The results of PCA of all genera (Fig. 2A) showed that the first two PCs accounted for 62.75% of the total variance of the original data set, of which PC1 explained 40.93% of the total variance and PC2 explained 21.82% of the total variance. PC1 indicates that the microbial composition is significantly different between the two fillers, and PC2 indicates that the microbial composition is significantly different under different time treatments, among which the X1-X4, X5-X9, D1-D3 and D4-D9 samples have similar microbial compositions, which may be due to changes in the microbial community structure caused by environmental factors (such as temperature, dissolved oxygen, etc.) with seasonal changes.

The results of PCA of functional bacteria (Fig. 2B) showed that the first two PCs accounted for 61.47% of the total variance of the original data set, of which PC1 explained 35.04% of the total variance and PC2

explained 26.43% of the total variance. PC1 indicates that the microbial composition was significantly different between the two fillers. PC2 indicates that the microbial composition of samples D1-D9 at different times was similar, while the microbial composition in the X filler group varied. This difference indicates that with the change of seasons, the microbial composition of functional bacteria in the D filler was stable, while the microbial composition of functional bacteria in the X filler was unstable. This is an important reason for the difference in the denitrification performance of the two fillers.

3.3 Microbial community composition

The relative abundances of phyla and genera in different treatments are shown in Fig. 3. The relative abundances of the top five phyla in the D material from small to large followed the order *Proteobacteria, Bacteroidetes, Firmicutes, Chloroflexi*, and *Verrucomicrobia*. The top five phyla in the X material from small to large followed the order *Proteobacteria, Bacteroidetes, Epsilonbacteraeota, Firmicutes*, and *Verrucomicrobia*. A total of 540 bacterial sequences in 18 samples were classified from 23732 OTUs. Within the D material, the main bacterial phyla were Proteobacteria (76%-51%) and Bacteroides (33%-15%), followed by *Firmicutes, Chloroflexus*, and *Verrucobacteria.* Within the X material, the main bacterial phyla were *Proteobacteria* (84%-46%) and *Bacteroides* (52%-7%), followed by *Epsilonbacteraeota, Firmicutes* and *Verrucomicrobia.* Among these phyla, *Chloroflexi* was more abundant in the D material, and *Epsilonbacteraeota* was more abundant in the X material (Fig. 3a-b).

At the genus level, the top ten genera of the D material were *Sphaerotilus, Thiothrix, Zoogloea, Flavobacterium, Buttiauxella, Enterobacter, Bacteroidetes_bacterium, Chryseobacterium, Gemmobacter*, and *Cloacibacterium.* The top ten genera of the X material were *Flavobacterium, Gemmobacter, Tolumonas, Aeromonas, Enterobacter, Cloacibacterium, Sphaerotilus, Buttiauxella, Vogesella*, and *Haliangium* (Fig. 3c-d). Among them, *Flavobacterium, Buttiauxella, Enterobacter, Gemmobacter, Cloacibacterium*, and *Sphaerotilus* were the common flora in all samples. *Zoogloea* and *Chryseobacterium* can secrete extracellular polymer substances, which promotes the formation of biological flocs and the stabilization of biofilms (Miao et al., 2017; Khani et al., 2016). The relative abundance of *Zoogloea* and *Chryseobacterium* in the D material was higher than that in the X material, which may be the reason for the more stable biofilm of the D material. *Aeromonas* is a psychrotrophic bacterium (Schubert et al., 2000). *Aeromonas* had a higher relative abundance in the X material than in the D material, indicating that the X material is more affected by temperature.

3.4. Analysis of the difference between dominant bacteria and functional bacteria on the surface of different materials

As part of the morphology of the biofilm carrier, pores not only increase the surface area of the biofilm but also provide a rich living environment for microorganisms. An appropriate pore structure enables sufficient mass transfer of oxygen and substrate. However, if the biofilm carrier used has a pore structure that is too small or too large, it will not be conducive to the improvement of reactor performance. A pore structure that is too small limits the mass transfer of oxygen to the substrate. A pore structure that is too large enhances the water shear force and reduces the stability of the biofilm. Holes larger than 1 mm can

not only increase the biomass of biofilms but also ensure sufficient mass transfer in the holes. Holes with irregular pore sizes larger than 1 mm can not only increase the biomass of biofilms but also provide a variety of environments, which are helpful for cultivating various cells and uneven biofilms. Therefore, SND can occur effectively (Al-Amshawee et al., 2020). The D material has 64 porous structures with a diameter of 2–4 mm, and the X material has 4 holes with a diameter of 4 mm. Our research results show that porous materials can create a microenvironment with different oxygen concentration gradients, which is suitable for the survival of different bacteria.

To reveal the differences in biofilm biomarkers on the surfaces of the two materials, LEfSe was performed on the top 20 dominant bacteria and functional bacteria of the two materials (Fig. 4A). The results showed that the microbial composition of the two fillers was significantly different. The difference analysis of dominant bacteria showed that *Sphaerotilus, Zoogloea, Thiothrix*, *Sphingobacteriales, Pseudomonas*, and *Fusibacter* were significantly enriched on the D material biofilm, while only *Haliangium* was significantly enriched on the X material.

The results of functional bacteria difference analysis (Fig. 4B) showed that on the D material biofilm, *Nitrosomonadaceae, Nitrospira, Azospira, Denitratisoma, Muricauda, Novosphingobium, Zoogloea*, and *Hydrogenophaga* were significantly enriched, while *Paracoccus* was significantly enriched on the X material biofilm.

Among the above genera, *Sphaerotilus, Sphingobacteriales, Pseudomonas, Nitrosomonadaceae, Nitrospira, Azospira, Hydrogenophaga*, and *Zoogloea* are more suitable for aerobic environments (Rattanachomsri et al., 2011; Wanner et al., 1987; Zhou et al., 2018). *Thiothri, Haliangium. Muricauda* and *Novosphingobium* are more suitable for anaerobic environments (Pang et al., 2018; Nielsen et al., 2000). *Paracoccus* is a facultative anaerobe (Medhi et al., 2017). Downing et al. (2008) showed that nitrite-oxidizing bacteria (NOB) and ammonia-oxidizing bacteria (AOB) have different sensitivities to DO, and the relative abundance of AOB does not differ greatly at different DO concentrations. NOB are more sensitive to DO and are more suitable for growth under high DO concentrations.

The D material biofilm could simultaneously enrich aerobic bacteria and anaerobic bacteria with different aerobic degrees, and the X material biofilm environment was more suitable for the survival of anaerobic bacteria and was not conducive to the enrichment of aerobic bacteria. This may be because the porous materials are in contact with DO in air and water, and the porous channel structures have different oxygen transfer capabilities, thereby creating biofilm microenvironments with different DO concentrations.

3.5. Stability analysis of functional bacterial communities of different materials

Analysis of the bacterial community structure showed that some bacteria in the reactor were involved in the denitrification process, and the functional bacteria are shown in Fig. 5A. The functional bacteria in the two systems were relatively consistent. The relative abundance of conventional autotrophic AOB was low and included only *Nitrosomonadaceae* (Pelissari et al., 2018; Kong et al., 2017), while heterotrophic AOB

included *Paracoccus, Acinetobacter, Pseudomonas, Hydrogenophaga* and *Acidovorax* (Lin et al., 2020). The NOB bacteria included *Nitrospira*. In addition, denitrifying bacteria were relatively abundant and included *Comamonas, Aeromonas, Azoarcus, Arcobacter, Azospira, Thiobacillus, Denitratisoma, Flavobacterium, Muricauda, Novosphingobium, Thaurea, Zoogloea* and *Rhodobacter* (Li et al., 2017; Huang et al., 2019; He et al., 2017; He et al., 2018). As shown in Fig. 5B, with decreasing temperature, the relative abundances of autotrophic AOB, heterotrophic AOB and NOB in the D material changed little with time, the species diversity and richness were large, and the relative abundance of functional bacteria remained basically stable. In the D material biofilm, autotrophic AOB mainly included *Nitrosomonadaceae*, heterotrophic AOB mainly included *Paracoccus, Acinetobacter, Hydrogenophaga*, and *Acidovorax*, and NOB mainly included *Nitrospira*. Denitrifying bacteria (DNB) mainly included *Zoogloea, Flavobacterium*, and *Arcobacter*. The relative abundances of autotrophic AOB, heterotrophic AOB and NOB on the X material were greatly affected by environmental changes. The relative abundance of functional bacteria changed greatly. Autotrophic AOB and NOB changed with decreasing temperature. In the X material biofilm, as the temperature decreased, the relative abundance of the autotrophic AOB *Nitrosomonadaceae* and NOB *Nitrospira* decreased, and the relative abundance of heterotrophic AOB increased. The genus with the greatest relative abundance in autumn was Pseudomonas, and the genera with the greatest relative abundance at lower temperatures in autumn and winter were mainly Pseudomonas and Acinetobacter. In the X material biofilm, DNB mainly included Flavobacterium at higher temperatures in summer and autumn, while *Aeromonas*, *Arcobacter, Flavobacterium*, and *Zoogloea* had the greatest relative abundances at lower temperatures in autumn and winter. The functional bacterial community structure of the D material biofilms showed stronger stability under the influence of environmental changes. *Pseudomonas* has low temperature tolerance, so it was relatively abundant in the two materials (Rashid et al., 2001).

3.6 Difference analysis of the stability and denitrification of functional bacteria with different materials

The results of Spearman correlation analysis between functional bacteria and environmental factors are shown in Fig. 6A and Table 5. Functional bacteria were greatly affected by environmental factors. The main environmental factors that affected functional bacteria were the specific surface area, number of pores, pore depth of the material, and temperature. It can be seen from the figure that the specific surface area and number of pores were positively correlated with aerobic autotrophic AOB (*Nitrosomonadaceae*), NOB (*Nitrospira*), and heterotrophic AOB (*Azospira, Hydrogenophaga*). The specific surface area and number of pores were positively correlated with the anaerobic bacterium *Denitratisoma*. However, pore depth was negatively correlated with *Nitrospira, Azospira, Nitrosomonadaceae, Denitratisoma, Muricauda*, and *Rhodobacter*. This may be because the deeper the pores are, the less favourable the mass transfer process of oxygen between the biofilm and the air and water, which is likely to cause an anaerobic environment. This finding also verifies the hypothesis that the special specific surface area and pore structure of the D material will create different anaerobic and aerobic environments. Temperature also significantly affected functional bacteria. Temperature changes were inversely related to changes in the relative abundance of *Aeromonas, Arcobacter*, and *Zoogloea.* Studies have shown that *Aeromonas* has

high biological activity at 4–37°C (Mizan et al., 2018; Nagar et al., 2017), and most strains still have high vitality at low temperature (10°C). Gonzalez-Martinez et al. (2018) used Arctic sludge to inoculate an AGS bioreactor and operated it in a temperature range of 3–7°C. The functional strains *Zooglea, Arcobacter* and *Acinetobacter* were all dominant, which is consistent with the results of this study.

Table 5 Correlation analysis between functional bacteria and environmental factors

Functional bacteria	Environmental Factors	R	P
Nitrospira	Number of holes	0.85	0.01
Azospira	Number of holes	0.89	0.02
Nitrospira	Specific surface area	0.85	0.01
Azospira	Specific surface area	0.89	0.01
Aeromonas	Temperature	-0.73	0.01
Nitrosomonadaceae	Number of holes	0.68	0.02
Denitratisoma	Number of holes	0.69	0.02
Nitrosomonadaceae	Specific surface area	0.68	0.02
Denitratisoma	Specific surface area	0.69	0.03
Arcobacter	Temperature	-0.67	0.01
Zoogloea	Temperature	-0.63	0.01
Hydrogenophaga	Number of holes	0.8	0.01
Hydrogenophaga	Specific surface area	0.8	0.01
Nitrospira	Pore depth	-0.85	0.01
Azospira	Pore depth	-0.89	0.02
Nitrosomonadaceae	Pore depth	-0.68	0.02
Denitratisoma	Pore depth	-0.69	0.01
Muricauda	Pore depth	-0.61	0.01
Rhodobacter	Pore depth	0.57	0.01

From the results of correlation analysis, the functional bacteria of the D material had low correlation, and only *Pseudomonas* and *Comamonas* were negatively correlated (Fig. 6B and Table 6). The functional bacteria of the X material were relatively closely related to each other (Fig. 6C and Table 6); *Aeromonas* and *Arcobacter* were positively related to *Thaurea, Arcobacter* and *Thaurea* were negatively related to *Nitrospira* and *Flavobacterium, Arcobacter* was negatively related to *Novosphingobium*, and *Flavobacterium* was negatively related to Acinetobacter.

Table 6
D and X material functional bacteria correlation analysis

	Functional bacteria	Functional bacteria	R	P
X	Flavobacterium	Acinetobacter	-0.92	0.01
	Thauera	Flavobacterium	-0.91	0.01
	Thauera	Nitrospira	-0.86	0.03
	Thauera	Arcobacter	0.88	0.03
	Arcobacter	Aeromonas	0.84	0.04
	Nitrospira	Arcobacter	-0.86	0.04
	Flavobacterium	Arcobacter	-0.84	0.04
	Novosphingobium	Arcobacter	-0.84	0.04
D	Comamonas	Pseudomonas	-0.88	0.01

The temperature decreased with changes in season, resulting in higher levels of *Aeromonas, Arcobacter*, and *Zoogloea* in the system with the X material, while *Aeromonas* and *Arcobacter* led to an increase in the relative abundance of *Thaurea*, thereby inhibiting and reducing the relative abundance of NOB (*Nitrospira*) and *Flavobacterium*. The change in *Flavobacterium* caused an increase in *Acinetobacter* content. NOB is the main limiting factor for nitrogen removal (Chen et al., 2018). The instability of functional bacteria leads to poor and unstable denitrification performance. This is consistent with the description of the functional bacteria in Fig. 5B.

In summary, the D material has a large number of pores, creating spatially isolated biofilm microenvironments with different DO concentrations, reducing the interaction between microorganisms. Therefore, material D is not only suitable for the growth of various bacteria with different oxygen demand functions but also reduces the impact of environmental changes on the denitrification performance of the reactor during operation and enhances the stability of the denitrification performance of the reactor. The X material has a small number of pores, a relatively uniform microenvironment, and large interactions between functional bacteria. Changes in the external environment (especially temperature) cause a change in one strain, which in turn affects other strains, and the system shows poor stability.

Conclusion

This study investigated the SND performance of two polyethylene fillers with different specific surface areas and pore structures (flat and cylindrical) in RBCs with temperature changes. The results show that materials with a large specific surface area and porous channel structures not only increase the diversity and richness of microbial communities but also enhance the stability of the reactor's nitrogen removal performance with respect to seasonal changes. This may be because the material is in contact with DO in air and water, and the porous channel structure has different oxygen transfer capabilities, thereby

creating biofilm microenvironments with different DO concentrations. Each microenvironment is spatially isolated, which reduces interactions among microorganisms. Such interactions improved the stability of SND performance with temperature changes.

Declarations

Confict of Interest

The authors have no confict of interest.

Ethical Approval

Not applicable

Consent to Participate

Not applicable

Consent to Publish

Not applicable

Authors Contributions

Cheng Gao and Yi Chen design, performed experiments and writing the manuscript. ; Tianqi Ao and Qingpeng Guo draws the figures, writing the manuscript and performs some characterizations. Wenqing Chen provides lab facilities to conduct research and revised the manuscript.

Availability of data and materials

The materials were available subject to availability.

Funding section

Not applicable

References

1. Al-Amshawee S, Yunus MYBM (2020) Geometry of biofilm carriers: A systematic review deciding the best shape and pore size.Groundw. Sustain. Dev.100520
2. Bai L, Cui J, Jie W (2015) Analysis of the community compositions of rhizosphere fungi in soybeans continuous cropping fields[J]. Microbiol Res 180:49–56
3. Bassin JP, Dezotti M (2018) Moving bed biofilm reactor (MBBR)[M]//Advanced biological processes for wastewater treatment. Springer, Cham, pp 37–74

4. Bhattacharya R, Mazumder D (2021) Simultaneous nitrification and denitrification in moving bed bioreactor and other biological systems.Bioprocess.Biosyst. Eng.1–18
5. Chen M, Chen Y, Dong S (2018) Mixed nitrifying bacteria culture under different temperature dropping strategies: Nitrification performance, activity, and community[J]. Chemosphere 195:800–809
6. Chen Y, Lan S, Wang L (2017) A review: driving factors and regulation strategies of microbial community structure and dynamics in wastewater treatment systems[J]. Chemosphere 174:173–182
7. Cortez S, Teixeira P, Oliveira R (2008) Rotating biological contactors: a review on main factors affecting performance[J]. Rev Environ Sci Biotechnol 7(2):155–172
8. Dawson R, Murphy N, K, L (1972) The temperature dependency of biological denitrification[J]. Water Res 6(1):71–83
9. Dong Y, Chen Y, Guo J et al (2021) Treatment of mustard tuber wastewater (MTWW) using a pilot-scale packed cage rotating biological contactor system: process XXXodelling and optimization[J], vol 28. Environmental Science and Pollution Research, pp 32057–32065. 24
10. Downing L, Nerenberg S, R (2008) Effect of oxygen gradients on the activity and microbial community structure of a nitrifying, membrane-aerated biofilm[J]. Biotechnol Bioeng 101(6):1193–1204
11. Fang Q, Zhang C, Zhang K (2008) Effect of sludge age and pH value on simultaneous nitrification and denitrification (SND). Journal of Guangzhou University (Natural Science Edition
12. Franco-Frías E, Mercado-Guajardo V, Merino-Mascorro A (2021) Analysis of Bacterial Communities by 16S rRNA Gene Sequencing in a Melon-Producing Agro-environment. MICROB. ECOL, pp 1–10
13. Geng M, Ma F, Guo H et al (2020) Enhanced aerobic sludge granulation in a Sequencing Batch Reactor (SBR) by applying mycelial pellets[J]. J Clean Prod 274:123037
14. Gonzalez-Martinez A, Muñoz-Palazon B, Maza-Márquez P (2018) Performance and microbial community structure of a polar Arctic Circle aerobic granular sludge system operating at low temperature[J]. Bioresour Technol 256:22–29
15. Han Y, Ma J, Xiao B (2019) New integrated self-refluxing rotating biological contactor for rural sewage treatment[J]. J Clean Prod 217:324–334
16. He Q, Zhang W, Zhang S (2017) Performance and microbial population dynamics during stable operation and reactivation after extended idle conditions in an aerobic granular sequencing batch reactor[J]. Bioresour Technol 238:116–121
17. He S, Wang Y, Li C (2018) The nitrogen removal performance and microbial communities in a two-stage deep sequencing constructed wetland for advanced treatment of secondary effluent[J]. Bioresour Technol 248:82–88
18. Hocaoglu SM, Insel G, Cokgor EU (2011) Effect of low dissolved oxygen on simultaneous nitrification and denitrification in a membrane bioreactor treating black water[J]. Bioresour Technol 102(6):4333–4340

19. Huang J, Cao C, Liu J (2019) The response of nitrogen removal and related bacteria within constructed wetlands after long-term treating wastewater containing environmental concentrations of silver nanoparticles[J]. Sci Total Environ 667:522–531
20. Iannacone F, Di Capua F, Granata F et al (2020) Simultaneous nitrification, denitrification and phosphorus removal in a continuous-flow moving bed biofilm reactor alternating microaerobic and aerobic conditions[J]. Bioresour Technol 310:123453
21. Khani M, Bahrami A, Chegeni A (2016) Optimization of carbon and nitrogen sources for extracellular polymeric substances production by Chryseobacterium indologenes MUT. 2[J]. Iran J BIOTECHNOL 14(2):13
22. Kiran M, Pakshirajan G, Das K, G (2017) A new application of anaerobic rotating biological contactor reactor for heavy metal removal under sulfate reducing condition[J]. Chem Eng J 321:67–75
23. Kong Q, He X, Ma S (2017) The performance and evolution of bacterial community of activated sludge exposed to trimethoprim in a sequencing batch reactor[J]. Bioresour Technol 244:872–879
24. Li N, Zeng W, Yang Y et al (2019) Oxygen mass transfer and post-denitrification in a modified rotating drum biological contactor[J]. Biochem Eng J 144:48–56
25. Li X, Sun S, Yuan H (2017) Mainstream upflow nitritation-anammox system with hybrid anaerobic pretreatment: long-term performance and microbial community dynamics[J]. Water Res 125:298–308
26. Li YF, Peng L, Ngo HH, Guo WS, Wang DB, Pan YT, Sun J, Ni BJ (2016) Evaluation of nitrous oxide emission from sulfide- andsulfur-based autotrophic denitrification process. Environ Sci Technol 50(17):9407–9415
27. Lin Z, Huang W, Zhou J (2020) The variation on nitrogen removal mechanisms and the succession of ammonia oxidizing archaea and ammonia oxidizing bacteria with temperature in biofilm reactors treating saline wastewater[J]. Bioresour Technol 314:123760
28. Luo Z, Wang D, Yang J (2020) The effect of using pig manure as an internal carbon source in a traditional piggery wastewater treatment system for biological denitrification[J]. Ecol Eng 143:105638
29. Ma W, Han Y, Ma W et al (2019) Simultaneous nitrification and denitrification (SND) bioaugmentation with Pseudomonas sp. HJ3 inoculated for enhancing phenol and nitrogen removal in coal gasification wastewater[J]. Water Sci Technol 80(8):1512–1523
30. Medhi K, Singhal A, Chauhan D, K (2017) Investigating the nitrification and denitrification kinetics under aerobic and anaerobic conditions by Paracoccus denitrificans ISTOD1[J]. Bioresour Technol 242:334–343
31. Miao L, Wang C, Hou J (2017) Response of wastewater biofilm to CuO nanoparticle exposure in terms of extracellular polymeric substances and microbial community structure[J]. Sci Total Environ 579:588–597
32. Mizan M, F R, Jahid I, Park K, S, Y (2018) Effects of temperature on biofilm formation and quorum sensing of Aeromonas hydrophila[J]. Ital J Food Saf 30:456–466

33. Nagar V, Pansare, Godambe L, Bandekar J, R (2017) Biofilm formation by Aeromonas strains under food-related environmental stress conditions[J]. J Food Process Preserv 41(5):13182
34. Nielsen P, De H, Muro M, Nielsen A, J, L (2000) Studies on the in situ physiology of Thiothrix spp. present in activated sludge[J]. Environ Microbiol 2(4):389–398
35. Pang H, Zhou Z, Niu T (2018) Sludge reduction and microbial structures of aerobic, micro-aerobic and anaerobic side-stream reactor coupled membrane bioreactors[J]. Bioresour Technol 268:36–44
36. Pelissari C, Guivernau M, Viñas M (2018) Effects of partially saturated conditions on the metabolically active microbiome and on nitrogen removal in vertical subsurface flow constructed wetlands[J]. Water Res 141:185–195
37. Rashid N, Shimada Y, Ezaki S (2001) Low-temperature lipase from psychrotrophic Pseudomonas sp. strain KB700A[J]. Appl Environ Microbiol 67(9):4064–4069
38. Rattanachomsri U, Kanokratana P, Eurwilaichitr L (2011) Culture-independent phylogenetic analysis of the microbial community in industrial sugarcane bagasse feedstock piles[J]. Biosci Biotechnol Biochem 75(2):232–239
39. Schubert RHW, Schubert RHW (2000) Intestinal cell adhesion and maximum growth temperature of psychrotrophic aeromonads from surface water[J]. INT J HYG ENVIR HEAL 203(1):83–85
40. Siripong S, Rittmann BE (2007) Diversity study of nitrifying bacteria in full-scale municipal wastewater treatment plants. Water Res 41:1110–1120
41. Spasov E, Tsuji J, Hug M, L, A (2020) High functional diversity among Nitrospira populations that dominate rotating biological contactor microbial communities in a municipal wastewater treatment plant[J]. ISME J 14(7):1857–1872
42. Teng J, Shen L, Xu Y et al (2020) Effects of molecular weight distribution of soluble microbial products (SMPs) on membrane fouling in a membrane bioreactor (MBR): Novel mechanistic insights[J]. Chemosphere 248:126013
43. Wang DB, Wang YL, Liu YW, Ngo HH, Lian Y, Zhao JW, Chen F, Yang Q, Zeng GM, Li XM (2017) Review: is denitrifying anaerobic methane oxidation-centered technologies a solution for the sustainable operation of wastewater treatment plants? Bioresour Technol 234:456–465
44. Wang J, Gong B, Wang Y (2017) The potential multiple mechanisms and microbial communities in simultaneous nitrification and denitrification process treating high carbon and nitrogen concentration saline wastewater[J]. Bioresour Technol 243:708–715
45. Wang J, Rong H, Cao Y (2020) Factors affecting simultaneous nitrification and denitrification (SND) in a moving bed sequencing batch reactor (MBSBR) system as revealed by microbial community structures.Bioprocess. Biosyst Eng 43:1833–1846
46. Wanner J, Chudoba J, Kucman K (1987) Control of activated sludge filamentous bulking—VII. Effect of anoxic conditions[J]. Water Res 21(12):1447–1451
47. Waqas S, Bilad M, Aqsha R, A (2021) Effect of membrane properties in a membrane rotating biological contactor for wastewater treatment[J]. J Environ Chem Eng 9(1):104869

48. Waqas S, Bilad M, Man R, Z, B (2021) An energy-efficient membrane rotating biological contactor for wastewater treatment[J]. J Clean Prod 282:124544
49. Waqas S, Bilad M, Man R, Z, B (2021) An energy-efficient membrane rotating biological contactor for wastewater treatment[J]. J Clean Prod 282:124544
50. Waqas S, Bilad M, R (2019) A review on rotating biological contactors[J]. Indones J Sci Technol 4(2):241–256
51. Xie X, Liu N, Ping J (2018) Illumina MiSeq sequencing reveals microbial community in HA process for dyeing wastewater treatment fed with different co-substrates[J]. Chemosphere 201:578–585
52. Yang L, Ren Y, Liang X, X (2015) Nitrogen removal characteristics of a heterotrophic nitrifier Acinetobacter junii YB and its potential application for the treatment of high-strength nitrogenous wastewater[J]. Bioresour Technol 193:227–233
53. Yuan J, Dong W, Sun F (2018) Low temperature effects on nitrification and nitrifier community structure in V-ASP for decentralized wastewater treatment and its improvement by bio-augmentation[J]. Environ Sci Pollut Res 25(7):6584–6595
54. Zhimiao Z, Xiao Z, Zhufang W (2019) Enhancing the pollutant removal performance and biological mechanisms by adding ferrous ions into aquaculture wastewater in constructed wetland[J]. Bioresour Technol 293:122003
55. Zhong D, Zhu K, Ma W (2021) Optimization of a Completely Mixed Anaerobic Biofilm Reactor (CMABR), Based on Brewery Wastewater Treatment. Water 13(5):606
56. Zhou SL, Zhang YR, Huang TL et al (2018) In Situ Nitrogen Removal by a Newly Isolated Oligotrophic Aerobic Denitrifier Zoogloea sp. N299, in Relations with Temperature and Water Pressure in a Reservoir[J].
57. Zhou X, Liang C, Jia L (2018) An innovative biochar-amended substrate vertical flow constructed wetland for low C/N wastewater treatment: impact of influent strengths[J]. Bioresour Technol 247:844–850

Figures

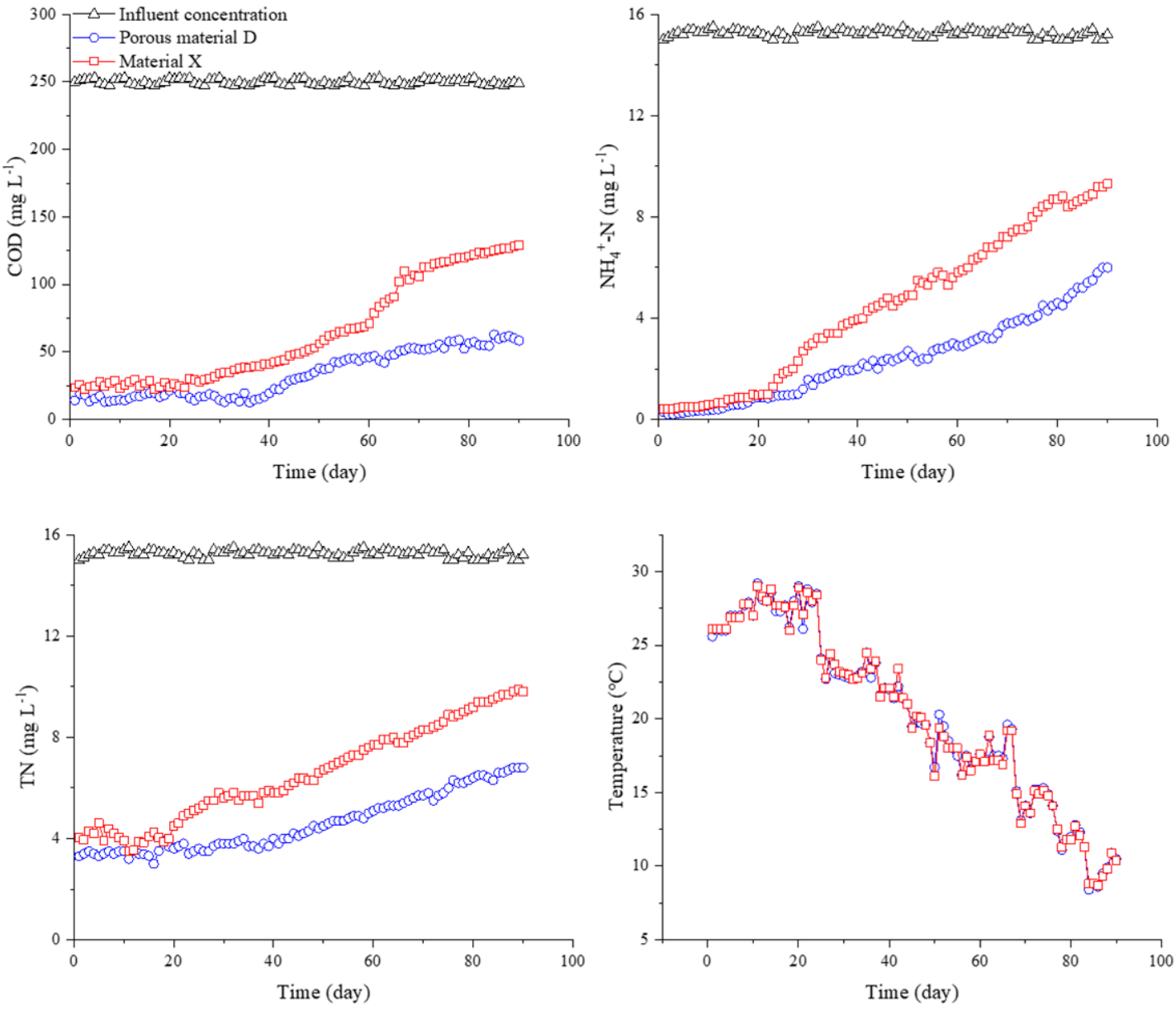

Figure 1

Outlet water quality

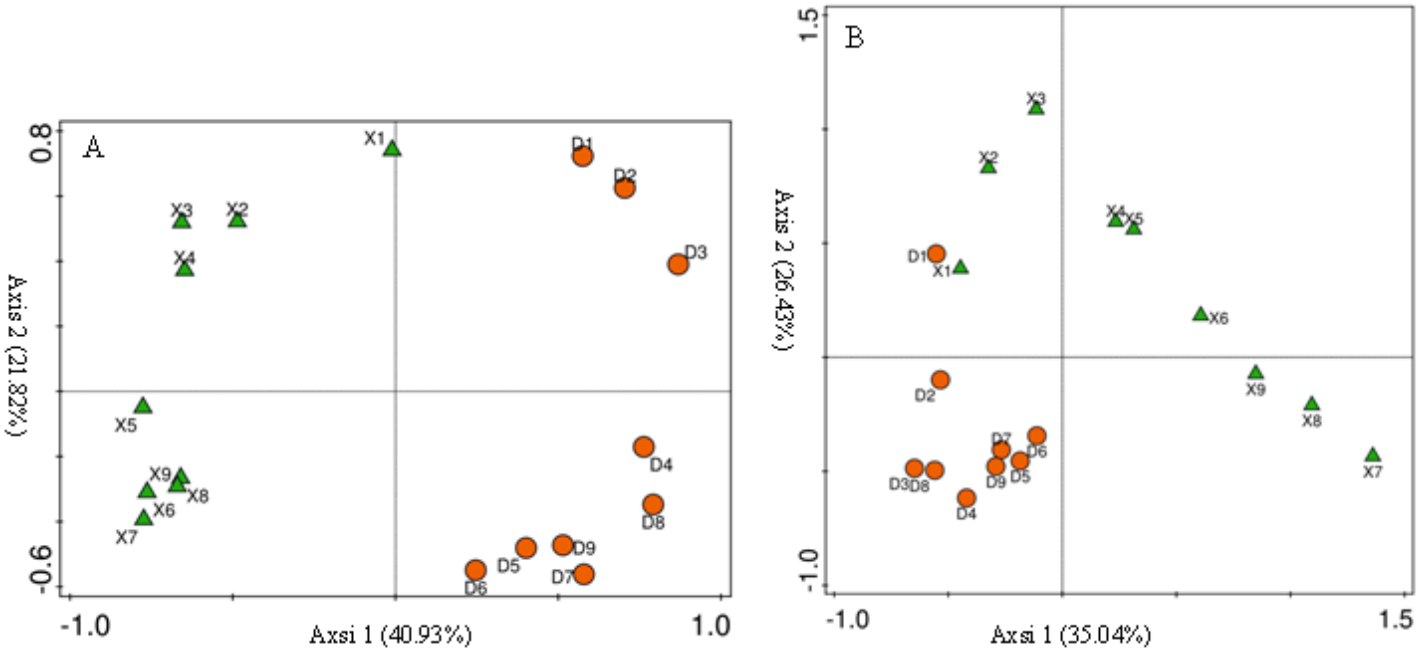

Figure 2

Principal component analysis of all genera (A); principal component analysis of functional bacteria (B)

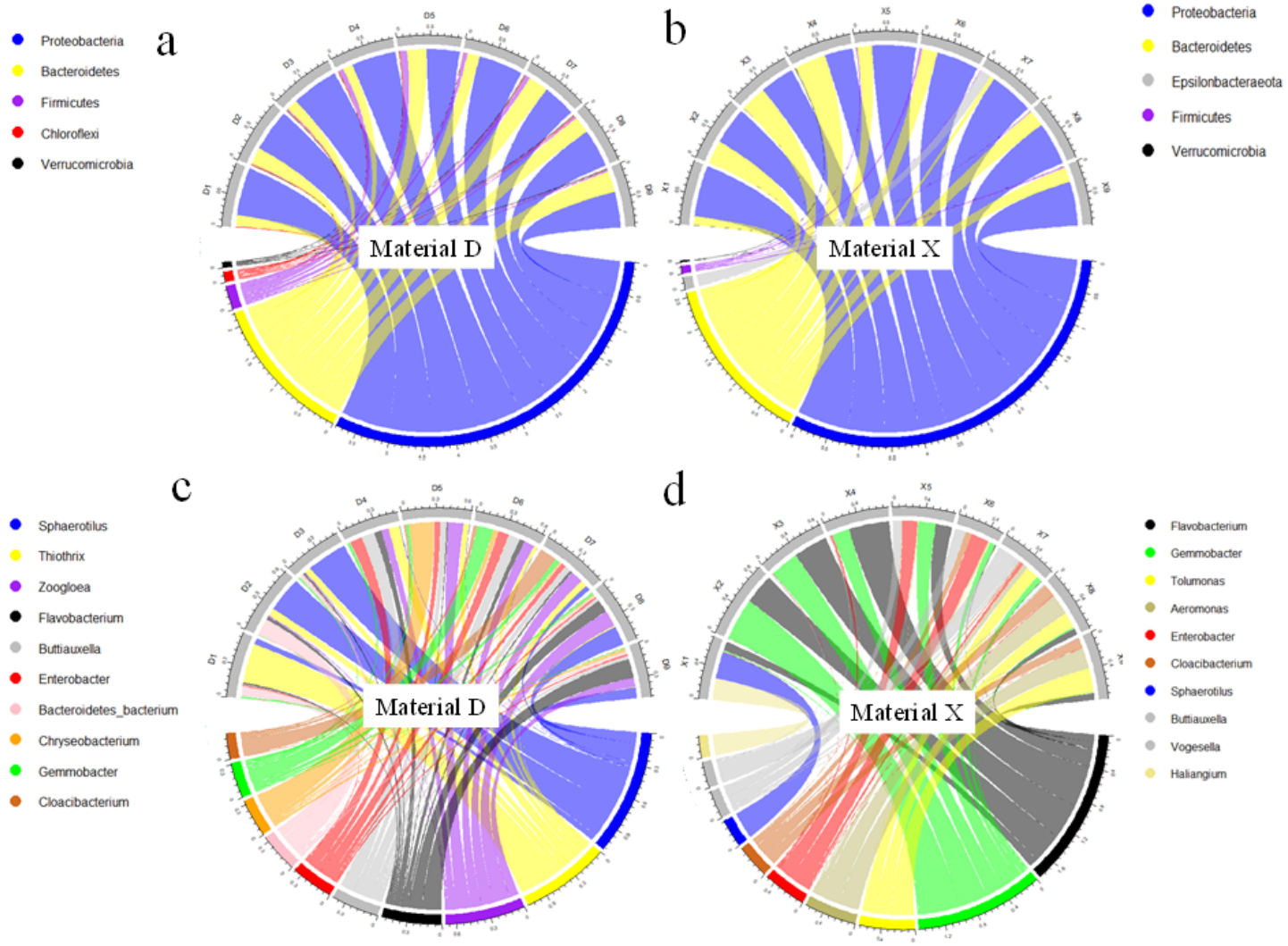

Figure 3

Relative abundance

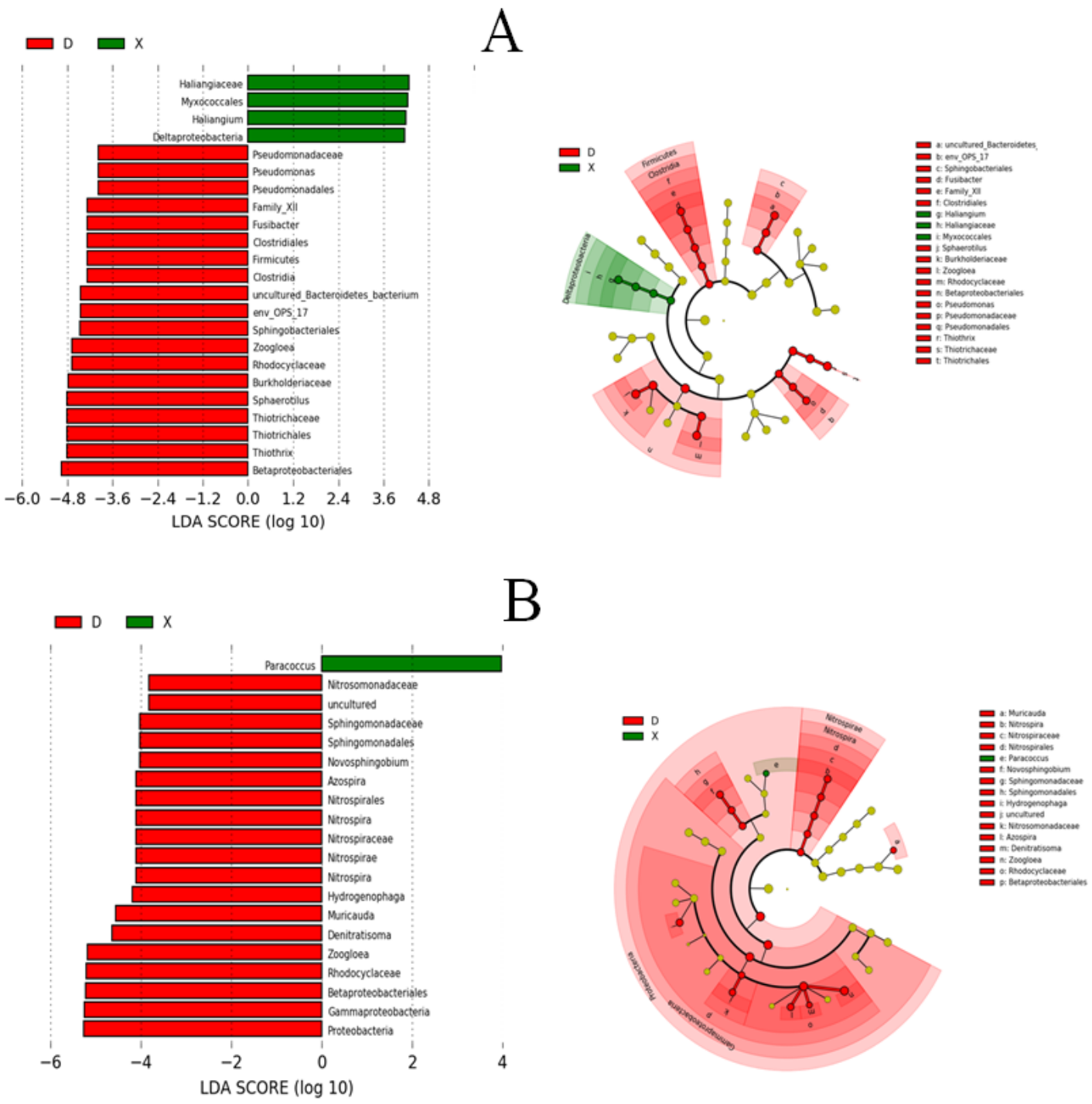

Figure 4

Difference analysis results

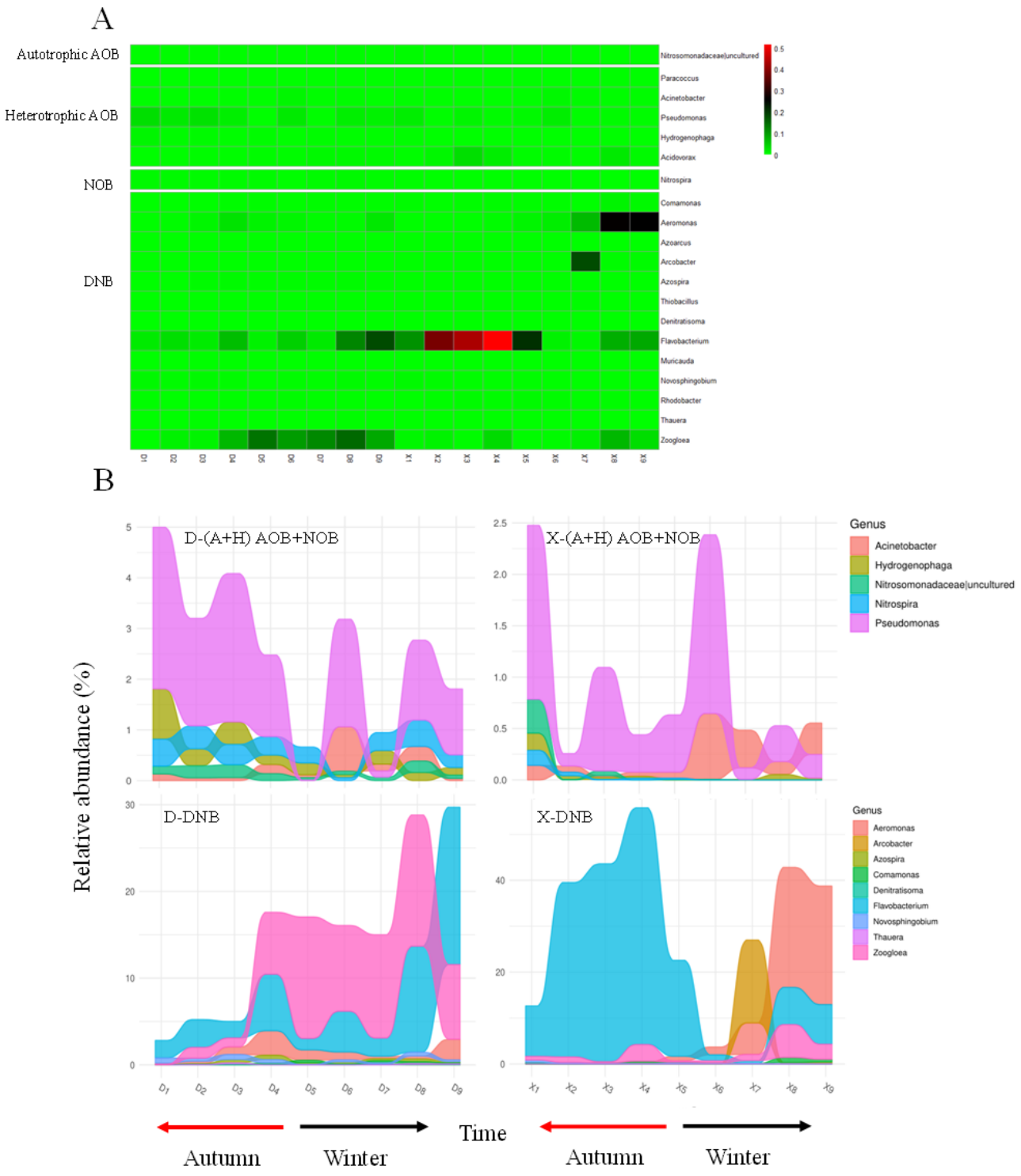

Figure 5

Relative abundance of functional bacteria (A); relative abundance of functional bacteria with varying seasons (B)

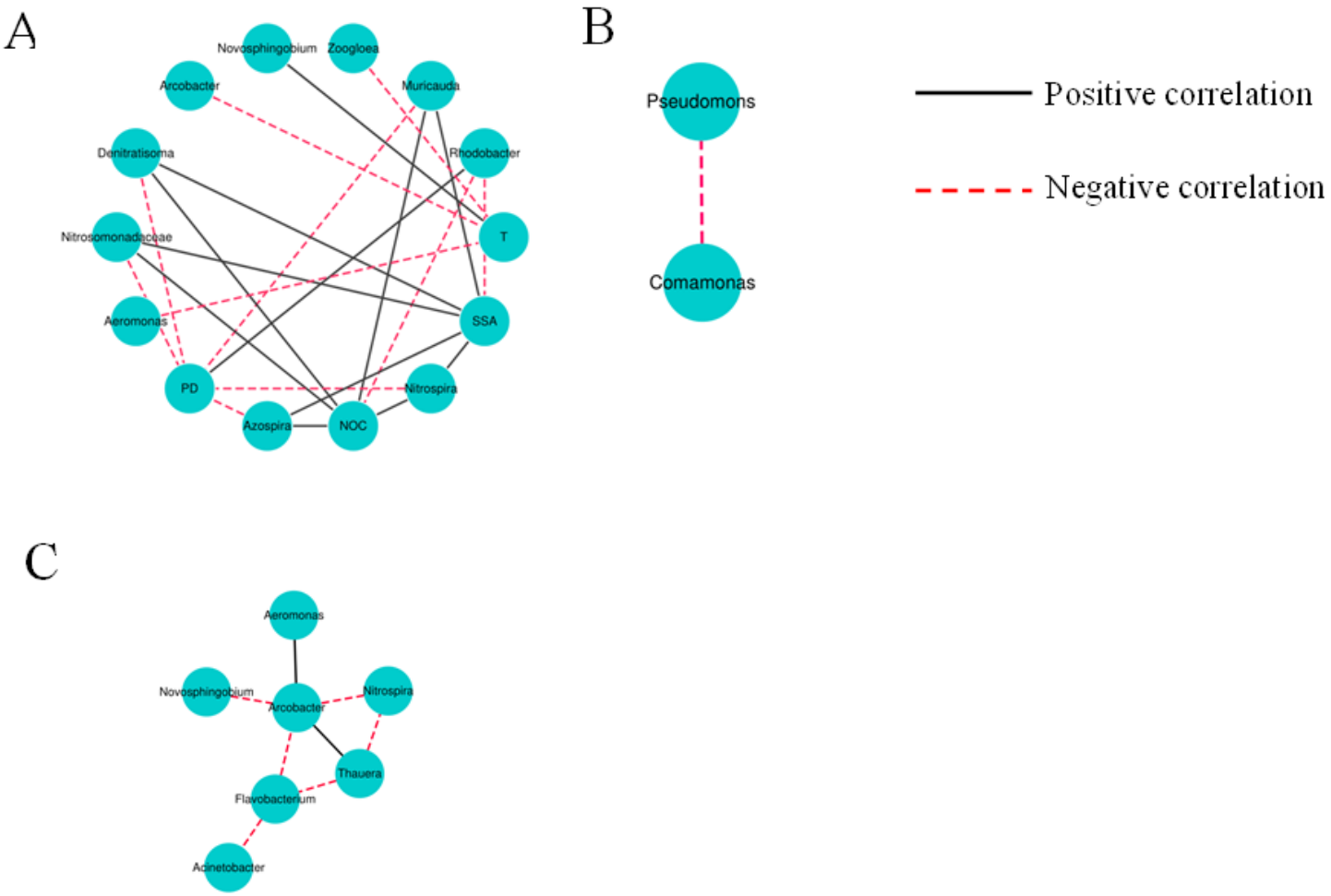

Figure 6

Correlation analysis between functional bacteria and environmental factors (A); D material functional bacteria correlation analysis (B); X material functional bacteria correlation analysis (C). T, temperature; SSA, specific surface area; NOC, number of holes; PD, pore depth.

Supplementary Files

This is a list of supplementary files associated with this preprint. Click to download.

- GraphicalAbstracts.docx
- Supplementarymaterial.docx